A Wideband 1.5-bit unit cell for Reconfigurable Reflectarray design

Leiyuan Qin*, Wei Hu*, Qi Luo‡, Rafael Caldeirinha§
*National Key Laboratory of Radar Detection and Sensing, Xidian University, Xi'an, China, weihu.xidian@ieee.org
‡School of Physics, Engineering and Computer Science, University of Hertfordshire, Hatfield, UK, qiluo@ieee.org
§Polytechnic of Leiria, Leiria, Portugal; Instituto de Telecomunicações, Leiria, Portugal, rafael.caldeirinha@ipleiria.pt

***Abstract*—This paper presents a low-complexity, wideband unit cell design suitable for reconfigurable reflectarrays (RRAs). To overcome the challenges of high implementation complexity associated with high-bit quantization, and the performance degradation resulting from one-bit quantization, a 1.5-bit phase quantization approach is proposed. The developed unit cell can operate in multiple modes to realize reflection phase delay, resonance tuning, and true-time delay, controlled by two PIN diodes. By switching the states of these diodes, the unit cell provides four reflection states. Wideband operation is achieved by selecting appropriate states across the frequency range to ensure continuous phase coverage. To validate the proposed concept, a unit cell was designed and simulated. The simulation results demonstrate stable three-phase responses with low reflection amplitude variation under different incidence angles across the 13.4–19.2 GHz frequency band.**

***Index Terms*—Reflectarray, metasurface, 1.5-bit, wideband, reconfigurable.**

I. Introduction

The application of reconfigurable reflectarray (RRA) in the next generation mobile communication [1], satellite communication [2], remote sensing [3], and other fields has attracted much attention. The RRA combines the advantages of traditional phased array and parabolic antenna, and has the characteristics of high gain, real-time beam agility and low complexity [4], [5], [6].

Tunable devices or materials such as p-i-n diodes, varactors, MEMS switches, and liquid crystals are used to achieve beam steering of the RRA. The varactor [7], [8] can achieve a continuous reflection phase range, but the insertion loss is large, the bias circuit is complex, and the voltage regulation accuracy is high. MEMS [9], [10] switches have advantages in low insertion loss, good electrostatic control, and monolithic integration. However, the high cost and low switching response of MEMS components affect their large-scale implementation. Liquid crystals [11], [12] have attracted interest because of their transparency and mechanical flexibility, but they have large insertion losses and delays.

p-i-n diodes are widely used in the design of RRA due to their low insertion loss, fast switching response and low price. Although p-i-n diodes have many attractive characteristics, they can only provide discrete phase states, resulting in some quantization loss. Yang et al. [13] analyzed the phase error caused by discrete phases. The phase quantization loss of 1-bit, 2-bit and 3-bit phase discretization is about 3 dB, 0.6 dB and 0.2 dB, respectively. 1-bit RRA has received extensive attention and research because it can significantly reduce the design complexity [14], [15], [16]. In [14], an ultra-broadband RRA is presented, employing both the mirror-symmetry principle and a sub-wavelength mechanism. The design achieves a 3 dB gain bandwidth of 44.4% and a maximum aperture efficiency of 20.9%. In comparison, RRAs with 2-bit phase quantization possess improved performance in terms of reducing SLL and increasing aperture efficiency. The implementation of 2-bit RRA is similar to that of 1-bit RRA, where a reflection phase difference of 90° can be obtained when p-i-n diodes are switched between the ON and OFF states [17], [18], [19], [20]. In [20], a polarization-insensitive 2-bit RRA is proposed by integrating two pairs of orthogonal p-i-n diodes on the top layer, and a square-ring slot and a vertical slot are used to suppress the cross-polarization level. It achieved an aperture efficiency of 31.2% with a 3 dB gain bandwidth of 8.6%.

Generally speaking, more switching states require more p-i-n diodes, which increases the complexity of the unit cell design and the overall controlling circuit. Moreover, the achievable bandwidth of the phase delay of each phase state would also have an impact on the overall bandwidth of the RRA. To address these challenges, this paper presents a low-complexity RA unit cell design based on 1.5-bit phase quantization. The paper is organized as follows. Section II introduces the structure of the proposed 1.5-bit RRA unit cell. Section III presents the analysis of the unit cell performance under both vertical and oblique incidence. Section IV analytically calculates the radiation pattern of a 12×12 reflectarray. Section V concludes this paper.

II. Unit Cell Design

A. RRA Unit Cell Design

The configuration of the proposed 1.5-bit RRA unit cell is shown in Fig. 1. It is composed of four layers and three dielectric substrates. The aperture size is $0.44\lambda_0 \times 0.44\lambda_0$ at the center frequency, 16.5 GHz. The top layer is a rectangular patch with a U-shaped slot and a parasitic patch. The second layer is a rectangular patch and a square ring. A metalized via hole is used to connect the top and second layers. The use of U-slot loading enhances the design flexibility, and the double-layer metal patch forms a double resonance structure, which increases the phase shift bandwidth. One p-i-n diode is placed between the rectangular patch and the parasitic patch to change the phase shift of the unit cell. The third layer is the ground layer, which provides isolation between the DC bias lines and the receiving patch. The bottom layer includes a phase-shifting structure with one p-i-n diode and a fan-shaped open-end stub. Note that the two p-i-n diodes share a common ground, which reduces the complexity of the controlling circuit. The first and second dielectric substrates are FBM220 ($\varepsilon_r = 2.2$, $tan\delta =$ 0.01, h1= 0.5 mm, h2=1 mm). The third dielectric substrate is Rogers 4003 ($\varepsilon_r = 3.3$, $tan\delta = 0.027$, h3 =0.2 mm). A bonding layer with a thickness of 0.2 mm is used between these substrates. The MACOM MA4AGP907 p-i-n diodes are chosen for this design. The equivalent circuit of the pin diode is shown in Fig. 2. The diodes exhibit an on-state resistance $R_{on} = 4\Omega$ with series inductance $L_{on} = 110pF$, and off-state capacitance $C_{off} = 30pF$ with series inductance $L_{off} = 24fF$.

III. Reconfigurable Reflection phase

The developed unit cell uses two different modes to realize reflection phase delay, resonance tuning and true-time delay. Unlike conventional 2-bit RRA unit cells where all four states operate at the same frequency band, the present design has two states for dedicated high- and low-frequency operation, respectively, while maintaining the other two wideband operation states that cover the full operational bandwidth. Low insertion loss and stable 3-phase switching in all sub-bands are achieved in the design. This method enables the switching of three distinct phase states over a wide frequency range, resulting in the realization of a broadband 1.5-bit RRA unit cell design.

The scattering parameters of the unit cell were simulated in the high-frequency structure simulator (HFSS). The simulation setup employed periodic boundary conditions and a Floquet Port excitation. The p-i-n diodes are modeled using RLC boundaries for both ON and OFF states. The four working states of the cell are referred to as "state 1," "state 2," "state 3," and "state 4," when the two p-i-n diodes are switched between "ON" and "OFF" states. As shown in Table I, the four operating states correspond to the following diode configurations: State 1: both diodes OFF; State 2: PIN1 ON and PIN2 OFF; State 3: PIN1 OFF and PIN2 ON; State 4: both diodes ON. As shown, States 1 and 2 provide broadband coverage (13.4-19.2 GHz), while States 3 and 4 are dedicated to the high (16.5-19.2 GHz) and low (13.4-16.5 GHz) frequency sub-bands, respectively. The simulated results, including reflection amplitude and phase under normal and oblique incidence, are shown in Fig. 3. Through switching the four states and each time selecting three corresponding phase states to cover the desired frequency band, the unit cell exhibits a reflection amplitude better than -2.4 dB and supports stable three-phase switching in the frequency range of 13.4-19.2 GHz, as demonstrated in Fig. 3(a). Fig. 3(b) shows the simulated results of the unit cell when the incident angle of the electromagnetic wave varies within 30°. It can be seen that the phase and amplitude responses of the RRA unit cell are stable under different incident angles with a wide bandwidth.

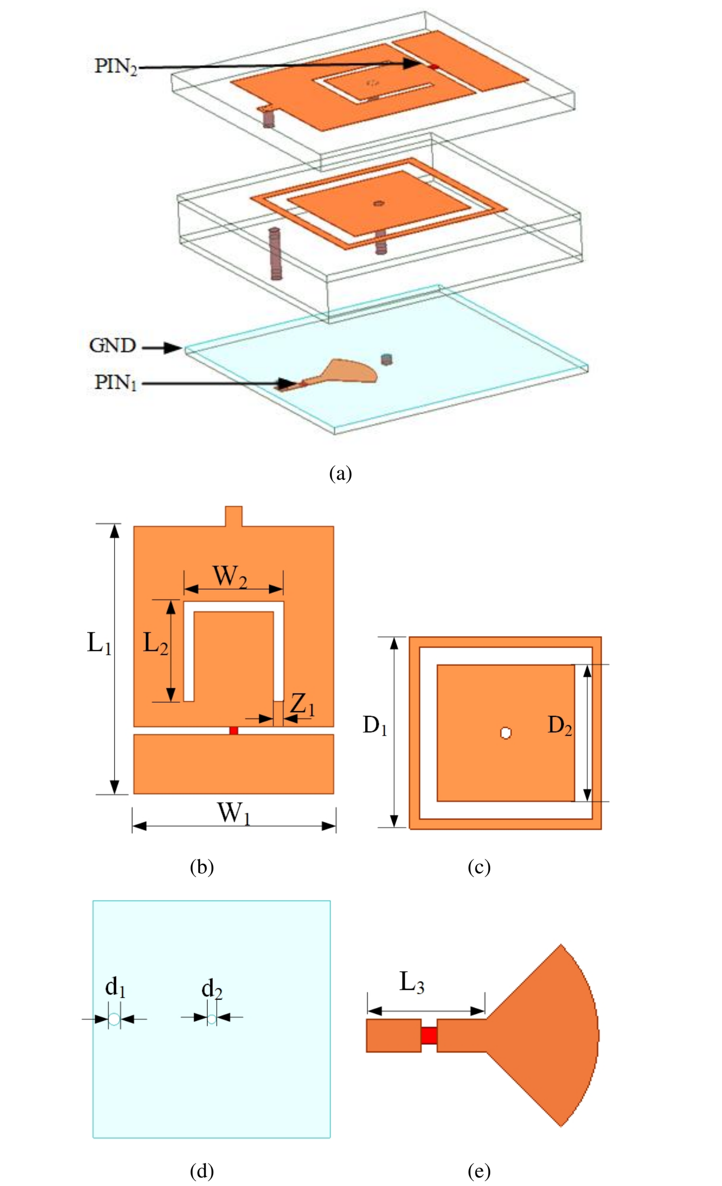

Fig. 1. The configuration of the proposed 3-phase cell: (a) exploded view, (b) first layer, (c) second layer, (d) third layer, and (e) fourth layer.

TABLE I
Operating States of the Proposed Unit Cell

State	PIN 1	PIN 2	Operating Mode	Frequency Range (GHz)
State 1	OFF	OFF	Original state	13.4–19.2
State 2	ON	OFF	Phase delay	13.4–19.2
State 3	OFF	ON	Resonance tuning	16.5–19.2
State 4	ON	ON	Resonance tuning	13.4–16.5

IV. Analytical Results

The response of a reflectarray consisting of 12×12 unit cells is analytically calculated by extracting the incident field

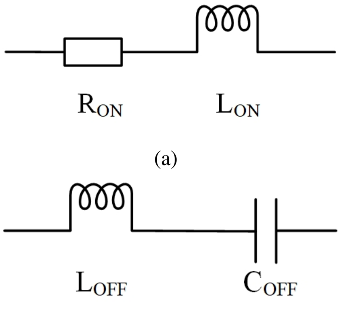

(b)

Fig. 2. Extracted equivalent circuit parameters of p-i-n diode at (a) ON state, (b) OFF state.

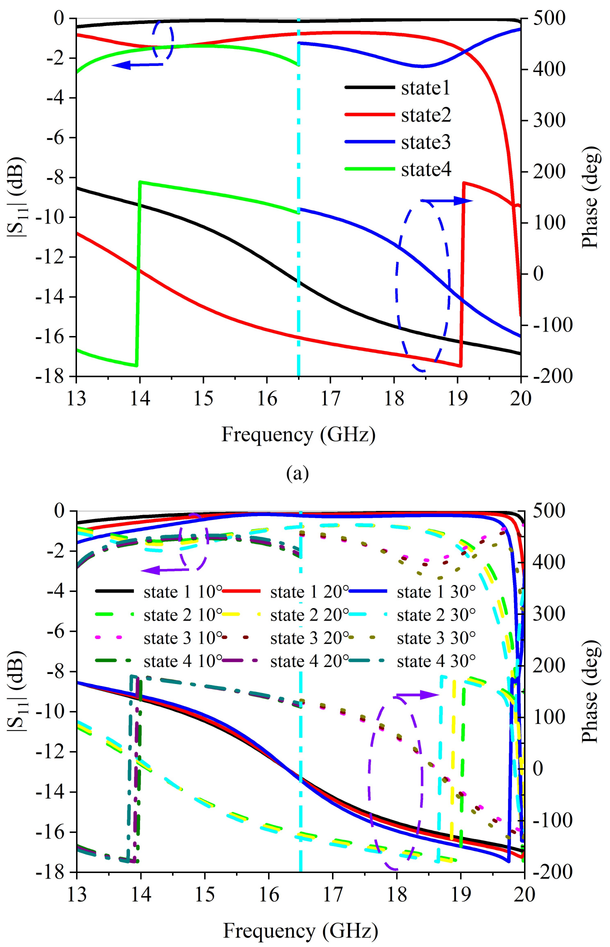

(b)

Fig. 3. Simulated reflection coefficients of the proposed RRA unit cell at (a) Vertical incidence, (b) Oblique incidence.

of the feed antenna and the radiation pattern of each unit cell. The calculated radiation pattern is presented in Fig. 4. The theoretical gains at 16 GHz and 17 GHz are 20.62 dBi and 20.68 dBi, respectively, with corresponding aperture efficiencies of 35% and 31.5%. The results demonstrate that the designed 1.5-bit reconfigurable unit cell increases the aperture efficiency of the array compared to conventional 1-bit

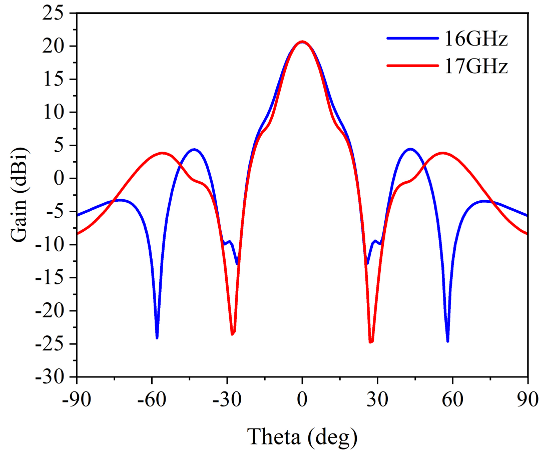

Fig. 4. Calculated radiation pattern of the reflectarray with 12×12 unit cells at 16GHz and 17GHz

designs.

V. Conclusion and Future Work

In conclusion, this paper proposes a wideband unit cell for RRAs. This unit cell ultilizes different operating modes to obtain phase delays in a wide frequency range, including two states for separate high- and low-frequency operation, while maintaining the other two states operating in the entire operational bandwidth. The simulation results show that the unit cell achieves a low reflection amplitude with stable phase switching over the frequency range of 13.4–19.2 GHz.

The future work of this study is to design and optimise the DC biasing line for the developed unit cell, and use full-wave EM simulations to validate the performance of the RRA before fabricating and measuring the prototype.

Acknowledgment

Dr Qi Luo and Prof. Rafael Caldeirinha would like to acknowledge the support from TERRAMETA project, which is funded by the Smart Networks and Services Joint Undertaking (SNS JU) under the European Union's Horizon Europe research and innovation programme under Grant Agreement No 101097101, including top-up funding by UK Research and Innovation (UKRI) under the UK government's Horizon Europe funding guarantee. This work is supported in part by the European Regional Development Fund (FEDER), through the Innovation and Digital Transition Programme (COMPETE 2030) of the Portugal 2030 framework [Project ALBATROZ with Nr. 17775 (COMPETE2030-FEDER-01335900)] and by Portugal PRR – Plano de Recuperacao e Resiliencia (The Recovery and Resilience Plan) under Project INOV.AM - Innovation in Additive Manufacturing.

References

[1] X. Cao, Q. Chen, T. Tanaka, M. Kozai, and H. Minami, "A 1-bit time-modulated reflectarray for reconfigurable-intelligent-surface applications," *IEEE Transactions on Antennas and Propagation*, vol. 71, no. 3, pp. 2396–2408, March 2023.

[2] K. Q. Henderson, W. Disharoon, and N. Ghalichechian, “Toward high-power beam-steerable reflectarrays using tunable-height dielectric,” *IEEE Transactions on Antennas and Propagation*, vol. 71, no. 3, pp. 2487–2496, March 2023.

[3] B. J, R. Scott, M. Nurnberger, H. Alqadah, B. Hicks, and K. Ackermann, “Mechanically-actuated reconfigurable reflectarray (marr) for microwave single pixel imager (mspi),” in *IGARSS 2020 - 2020 IEEE International Geoscience and Remote Sensing Symposium*, 2020, pp. 6547–6550.

[4] H. Yang *et al.*, “A 1600-element dual-frequency electronically reconfigurable reflectarray at x/ku-band,” *IEEE Transactions on Antennas and Propagation*, vol. 65, no. 6, pp. 3024–3032, June 2017.

[5] J. Han, L. Li, G. Liu, Z. Wu, and Y. Shi, “A wideband 1-bit 12x12 reconfigurable beam-scanning reflectarray: Design, fabrication, and measurement,” *IEEE Antennas and Wireless Propagation Letters*, vol. 18, no. 6, pp. 1268–1272, June 2019.

[6] H. Zhang, X. Chen, Z. Wang, Y. Ge, and J. Pu, “A 1-bit electronically reconfigurable reflectarray antenna in x band,” *IEEE Access*, vol. 7, pp. 66 567–66 575, 2019.

[7] A. Sayanskiy *et al.*, “A 2d-programmable and scalable reconfigurable intelligent surface remotely controlled via digital infrared code,” *IEEE Transactions on Antennas and Propagation*, vol. 71, no. 1, pp. 570–580, January 2023.

[8] C. Zhang, Y. Luo, N. Yan, K. Ma, and Z.-C. Hao, “A reconfigurable transmit-reflect-array antenna with arbitrary variable transmit-reflect function and continuous adjustable power ratio,” *IEEE Transactions on Antennas and Propagation*, vol. 73, no. 8, pp. 5610–5622, August 2025.

[9] K. Peng, B. Li, W. Yu, and X. Lv, “A 1-bit 110ghz mems-based beam-steerable reflectarray,” in *2022 International Conference on Microwave and Millimeter Wave Technology (ICMMT)*. IEEE, 2022, pp. 1–3.

[10] J. Tayebpour and R. R. Mansour, “Reconfigurable unit cell design using mems actuator for beam-steering applications,” *IEEE Transactions on Antennas and Propagation*, vol. 73, no. 3, pp. 1346–1354, March 2025.

[11] P. Aghabeyki, Y. Cai, G. Deng, Z. Tan, and S. Zhang, “A dual-polarized reconfigurable reflectarray with a thin liquid crystal layer and 2-d beam scanning,” *IEEE Transactions on Antennas and Propagation*, vol. 71, no. 4, pp. 3282–3293, April 2023.

[12] G. Deng, Y. Zhu, Q. Zhang, J. Yang, Y. Li, and Z. Yin, “Reconfigurable dual-functional reflective polarization converter based on liquid crystal terahertz metasurfaces,” *IEEE Transactions on Antennas and Propagation*, vol. 73, no. 6, pp. 4164–4169, June 2025.

[13] H. Yang *et al.*, “A study of phase quantization effects for reconfigurable reflectarray antennas,” *IEEE Antennas and Wireless Propagation Letters*, vol. 16, pp. 302–305, May 2017.

[14] J. Tian, S. Li, C. He, M. Premaratne, W. Zhu, and J. Zhou, “Ultrabroadband and multipolarized electrically reconfigurable reflectarray antennas,” *IEEE Transactions on Antennas and Propagation*, vol. 73, no. 2, pp. 723–732, February 2025.

[15] Z. Wang *et al.*, “1 bit electronically reconfigurable folded reflectarray antenna based on p-i-n diodes for wide-angle beam-scanning applications,” *IEEE Transactions on Antennas and Propagation*, vol. 68, no. 9, pp. 6806–6810, September 2020.

[16] H. Yang *et al.*, “A 1-bit 10×10 reconfigurable reflectarray antenna: Design, optimization, and experiment,” *IEEE Transactions on Antennas and Propagation*, vol. 64, no. 6, pp. 2246–2254, June 2016.

[17] Y. Yin *et al.*, “Design of a 2-bit dual-polarized reconfigurable reflectarray with high aperture efficiency,” *IEEE Transactions on Antennas and Propagation*, vol. 72, no. 1, pp. 542–552, January 2024.

[18] W. Li, H. Guo, X. Wang, G. Yang, and Y. Jin, “A 2-bit reconfigurable metasurface with real-time control for deflection, diffusion, and polarization,” *IEEE Transactions on Antennas and Propagation*, vol. 72, no. 2, pp. 1521–1531, February 2024.

[19] X. Ma *et al.*, “Design and rectangular waveguide validation of 2-bit wideband reconfigurable reflective metasurface element in x-band,” *IEEE Antennas and Wireless Propagation Letters*, vol. 22, no. 1, pp. 4–8, September 2023.

[20] Y. Chen *et al.*, “Design of 2-bit single linearly polarized reconfigurable intelligent surface for single-beam/multibeam scanning,” *IEEE Antennas and Wireless Propagation Letters*, vol. 23, no. 8, pp. 2366–2370, August 2024.